Scientific Reports

https://doi.org/10.1038/s41598-026-46890-3

Article in Press

Acid activated orange peel waste adsorbent for the elimination of phenol with insights into isotherm, kinetics, and thermodynamics

Received: 26 December 2025

Accepted: 27 March 2026

Published online: 02 April 2026

Cite this article as: Alqahtani Z., Kola O.E., Alsharif A. *et al.* Acid activated orange peel waste adsorbent for the elimination of phenol with insights into isotherm, kinetics, and thermodynamics. *Sci Rep* (2026). https://doi.org/10.1038/s41598-026-46890-3

Zahrah Alqahtani, Oladejo Emmanuel Kola, Aliyah Alsharif, Ali Shawabkeh, Afnan M. Alnajeebi, Roaa A. Tayeb, A. Al Solami, Hamad AlMohamadi & Jamelah S. Al-Otaibi

Acid activated orange peel waste adsorbent for the elimination of phenol with insights into isotherm, kinetics, and thermodynamics

[1]Zahrah Alqahtani, [2]Oladejo Emmanuel Kola, [3]Aliyah Alsharif, [4]Ali Shawabkeh, [5]Afnan M. Alnajeebi

,[6]Roaa A. Tayeb, [6]Amani Fahm Mohammed Al Solami, [7]Hamad AlMohamadi, and [8]Jamelah S. Al-Otaibi

[1]Physics Department, Faculty of Science, Taif University, Taif, P.O. Box 11099, Taif 21944, Saudi Arabia. [2]Department of Chemical Sciences, Mountain Top University, Prayer City, Ogun State, Nigeria.

[3]Department of Chemistry, Faculty of Science, Imam Muhammad Ibn Saud Islamic University, Riyadh 11564, Saudi Arabia.

[4]College of Engineering and Technology, American University of the Middle East, Kuwait.

[5]Department of Biological Sciences, College of Science, University of Jeddah, Jeddah, Saudi Arabia.

[6]Department of Chemistry, College of Science, University of Jeddah, Jeddah, Saudi Arabia.

[7]Department of Chemical Engineering, Faculty of Engineering, Islamic University of Madinah, Madinah, Saudi Arabia.

[8]Department of Chemistry, College of Science, Princess Nourah Bint Abdulrahman University, P.O. Box 84428, Riyadh 11671, Saudi Arabia

Abstract

This study explored the potential of acid-treated orange peel (ATOP) and raw orange peel (ROP) as sustainable, low-cost biosorbents for the elimination of phenol from aqueous solutions. Acid modification was employed to enhance the textural and surface chemistry properties of orange peel–derived biomass. Comprehensive characterization using FTIR, SEM, BET, and XRD confirmed successful surface functionalization, improved porosity, and structural modification after adsorption. The findings showed that ATOP demonstrated superior performance relative to ROP, achieving a maximum removal efficiency of 85.25% at 45 °C and reaching equilibrium within 150 min. The maximum adsorption capacities obtained from the Langmuir model were 80.32 mg g^{-1} for ROP and 133.13 mg g^{-1} for ATOP. Equilibrium data indicated Langmuir behavior for ROP and Freundlich behavior for ATOP, reflecting increased surface heterogeneity induced by activation. Kinetic assessment showed that phenol removal on ROP followed the pseudo-first-order model, while ATOP was best

explained by the pseudo-second-order model, signifying a shift toward stronger surface interactions after acid modification. Thermodynamic parameters established the process to be spontaneous and endothermic, with ΔH° values of 14.5 kJ mol^{-1} (ROP) and 45.32 kJ mol^{-1} (ATOP). Overall, the results demonstrate that acid-treated orange peel biomass is an efficient and environmentally benign adsorbent for phenol remediation in wastewater systems.

Keywords: Adsorption; Isotherm; Kinetics; Orange peel; Phenol; Wastewater

Corresponding author: *kolaoladejo7@gmail.com*

1.0 Introduction

Industrial effluents often contain phenol and its derivatives that originate from textile processing, petroleum refining, resin manufacturing and pharmaceuticals [1-2]. Wastewater containing large volumes of phenol and its derivatives is released annually, with reported concentrations ranging from trace levels to several thousand milligrams per liter. Because of their poor biodegradability, high toxicity, and persistence in aquatic environments, these contaminants pose severe threats to human health and ecosystems at large [2-3]. Rapid population growth, industrialization, and agricultural expansion have resulted in a considerable increase in phenolic compound emissions into the environment [4]. The discharge of phenol and its derivatives into water bodies has become a persistent environmental concern because of their high toxicity to the aquatic ecosystem, slow biodegradation, and ability to disrupt aquatic life even at low concentrations [5-6]. Prolonged contact with phenol can cause a wide range of severe health challenges such as skin burns, nerve damage, impaired vision, and gastrointestinal problems [3]. Exposure to phenol also adversely impacts vital human organs like the kidneys, liver, and central nervous system [7]. Phenolic compounds, including chlorophenols, are associated with serious health risks, including tissue damage, genetic damage, mutations, and cancer, threatening both human health and the ecosystem [6].

Commented [U1]:

Its persistence in water bodies could cause harm to aquatic life and disrupt the ecosystem due to oxygen depletion, which can have long-lasting effects on the environment [8]. Regulatory bodies like the United States Environmental Protection Agency (EPA) and the World Health Organization (WHO) consider phenol levels above 1 ppm a risk to human health and the environment [9]. Thus, the elimination of phenol from wastewater is vital to safeguard the environment from its hazardous effects. It also preserves aquatic life, protects human health, and promotes eco-friendly industrial processes. Developing cost-effective and sustainable phenol removal techniques is key to tackling phenol pollution and also creating cleaner water systems.

Conventional treatment procedures such as oxidation, membrane filtration, precipitation, and biological treatment are extensively used for the elimination of phenol from wastewater [10, 11]. These procedures often face some restrictions like high

operating cost, toxic by-products generation, complex process, and poor efficacy [12]. To address all these restrictions, adsorption appears as one of the most effective and versatile wastewater treatment methods because of its simplicity, high removal efficiency, environmental compatibility, and economic feasibility **[**3,13-14]. The effectiveness of the sorption procedures strongly depends on the characteristics of the adsorbent such as the availability of the material, binding groups present on its surface, enhanced surface area, and better pore structure [15].

Conventional adsorbents like activated carbon, silica gel, and polymer resins have been widely utilized for contaminant removal, and although they effectively remove pollutants, their high cost, limited reusability, inefficiency at removing low-concentration pollutants, and lower sustainability have prompted interest in alternative materials like biomass [15]. Activated carbon made from biomass, such as agricultural waste, offers a more eco-friendly and economical option with lower environmental impact due to its low cost and comparable performance, abundance of functional groups that facilitate the adsorption process, and porous structure [16]. Biomass-based adsorbents derived from agricultural and forestry wastes have recently gained considerable attention due to their renewability, abundance, and surface chemistry favorable for pollutant uptake **[**17-18**]**.

Agricultural waste such as corn cob [19], eucalyptus wood [20], sugarcane bagasse [21], and rice straw [22] have been used for effective elimination of phenol from wastewater. Among these adsorbents, orange peel represents one of the most promising yet underexplored biomass materials, generated in huge quantities as a by-product of citrus processing industries. Globally, orange peel waste generation exceeds 54 million metric tons annually [22], causing both an environmental burden and an opportunity for resource valorization. Therefore, converting orange peel waste into an effective adsorbent provides an environmentally responsible approach to valorizing biomass while addressing phenol pollution. Orange peel consists of pectin, cellulose, hemicellulose, and lignin, as well as surface functional groups that can interact strongly with pollutants such as phenol.

Chemical treatment, most especially acid activation, has been employed widely to improve the adsorption performance of biomass-based adsorbents by porosity, increasing surface acidity, and the availability of active binding sites, thereby enhancing affinity toward pollutants [14-18]. The orange peels which are lignocellulosic agro-wastes have gained significant interest as adsorbents because of their biodegradability, abundance, and richness in surface functional groups such as carboxyl, hydroxyl, and phenolic moieties. Nevertheless, the raw structure of the orange peel often limits its adsorption capacity because of low surface area, blocked pores, and limited accessibility of active sites. In overcoming these drawbacks, different chemical activation approaches have been employed, among which acid activation has proven to be effective because it increases active sites and surface functionality, improving

porosity and adsorptive behavior for organic pollutants and dyes [23-25]. Research conducted on citrus waste biomass, like orange peels, have shown that modification approaches enhanced contaminant sorption performance relative to raw materials [26]. Additionally, recent study on the preparation of activated char from orange peel demonstrated promising phenol adsorption capacities after chemical activation which was attributed to improved surface functionality, porosity as well as active sites [23, 27].

Although there have been reports of orange peel–derived adsorbents for contaminant uptake, most studies focus on a single modification route or provide limited mechanistic insight. In this study under the same experimental conditions, the study distinguishes itself by offering a direct and systematic comparison between raw orange peel (ROP) and acid-treated orange peel (ATOP) for phenol removal. This present work advances the previous understanding of citrus-waste–derived adsorbents by providing a systematic and mechanistically focused examination of acid modification effects on orange peel biomass. Unlike many earlier reports that evaluate either raw or modified materials in isolation, this study further integrates controlled side-by-side preparation, comprehensive physicochemical characterization (SEM, FT-IR, BET, XRD, and pH_{pzc}), and multi-model adsorption analysis to examine how mild acid activation changes surface chemistry, pore architecture, and adsorption pathways. By explicitly linking structural evolution to adsorption mechanism, the research offers deeper insight into the structure–function relationships governing phenol uptake on lignocellulosic adsorbents and provides a rational basis for tailoring low-cost biomass materials for wastewater remediation. In this study, the adsorption potentials of raw and acid-treated orange peel biomass towards phenol elimination from aqueous solutions were carefully examined by evaluating the effects of solution pH, contact time, temperature, adsorbent dosage, and initial phenol concentration. Adsorption kinetics, equilibrium isotherms, and thermodynamic analyses were employed to elucidate the governing adsorption mechanisms and assess the feasibility of acid-treated orange peel as a sustainable adsorbent for wastewater remediation. These details offer new insights into the impact of acid treatment in tailoring biomass-derived adsorbents for efficient phenol remediation.

2.0 Materials and methods

2.1 Materials

Analytical-grade sodium hydroxide (NaOH, 98%), phenol, and hydrochloric acid (HCl, 37%) were obtained from Sigma-Aldrich, India, and used for the preparation of solutions and pH adjustment. Distilled water served as the solvent for all dilutions.

2.2 Preparations of ATOP and ROP

Fresh orange peels (OP) were obtained from a local fruit market at Ibafo, Ogun State, Nigeria. Distilled water was used to thoroughly clean the peels to eliminate dirt and soluble impurities. The peels were reduced into smaller fragments and dried in an oven at 70 °C to eliminate the moisture content and labeled as ROP. Acid modification was carried out by soaking 20 g of the dried orange peel powder in 500 mL of 0.1 M HCl and left for 24 h with continuous stirring on an orbital shaker to allow proper acid activation. Hydrochloric acid was chosen as the activating agent due to the fact that it

provides an effective yet mild chemical modification route for lignocellulosic biomass. Compared to strong dehydrating acids like H_3PO_4 or salt-based activating agents like $ZnCl_2$ that often require high-temperature carbonization and extensive post-treatment, HCl primarily facilitates demineralization, partial hydrolysis of hemicellulose, and protonation of surface oxygenated groups under relatively mild conditions. This treatment can enhance surface acidity, expose previously blocked pores, and increase the accessibility of functional groups without causing severe structural collapse of the biomass matrix. In addition, HCl is inexpensive, readily available, easily removable by washing, and generates fewer secondary environmental concerns compared with heavy-metal chlorides such as $ZnCl_2$. After treatment, the sample was cleaned with distilled water repeatedly until the pH become neutral. The material was dried again and stored in airtight containers and labeled as (ATOP) for further use.

2.3 Characterization of the Adsorbent

Fourier transform infrared (FT-IR) study was carried out to establish the binding groups present on the biomass surface before and after phenol uptake. Dried and grounded fine powder of the adsorbent was mixed with potassium bromide (KBr) to produce pellets after compression. The spectra were recorded using FT-IR spectrophotometer (PerkinElmer Spectrum 2, USA) within the range of 400 to 4000 cm^{-1}. Scanning electron microscope (JEOL JSM-5600, Tokyo, Japan) was utilized to examine the morphology and textural features of the biomass. Small amounts of each sample were mounted on aluminum stubs with adhesive tape and coated with a thin layer of gold to enhance conductivity. The micrographs were obtained at different magnifications using a scanning electron microscope. The point of zero charge (pH_pzc) of raw- and acid-activated orange peel was estimated by adopting the pH-drift method. Briefly, 25 mL of 0.01 M NaCl solutions were adjusted to initial pH values in the range of 2 to 8. Afterward, 5 mg of biomass was introduced to each solution, and the suspensions were agitated for 12 h at 150 rpm. The final pH values were computed by obtaining the difference between the initial and final pH ($\Delta pH = pH_f - pH_0$) and plotted against the initial pH (pH_0) to obtain the pH_pzc. The Brunauer–Emmett–Teller (BET) instrument was employed for the determination of the surface area and pore size distribution with a Quantachrome NOVA 2200C instrument (USA). The crystalline and amorphous nature of the adsorbent was examined with X-ray diffraction (Bruker D8 Advance, Germany) equipped with Cu-Kα radiation (λ = 1.5406 Å) operated at 30 mA and 40 kV. Finely powdered samples were placed on a sample holder and scanned over a 2θ range of 5–50°.

2.4 Preparation of Phenol Solutions

A phenol stock solution was made by immersing 1 g of phenol in 1000 mL of distilled water to obtain a 1000 mg/L concentration. Desired working concentration solutions between 50 to 300 mg/L were made via serial dilution of the stock solution. The required pH value of each solution was determined via dilution with HCl or NaOH.

2.5 Batch Adsorption Experiments

Batch sorption studies were performed to examine the impacts of several experimental conditions and the study was performed in triplicate, while the mean values were

reported. In a typical run, a known mass of the orange peel adsorbents (5 - 40 mg) were added to 25 mL of phenol solution of known concentration (50 - 300 mg/L) in a series of conical flasks set-up, and the pH was regulated with either 0.1 M of NaOH or HCl. The content was reacted together following continuous agitation on a rotatory orbital shaker set at 150 rpm. At fixed time intervals (5 - 300 min), samples were taken, filtered, and the residual phenol concentration was analyzed with a UV-Vis spectrophotometer (Shimadzu UV-3600 UV-Vis-NIR spectrophotometer). The percentage removal (%R) and the phenol amount adsorbed (q_e) were determined using equations 1 and 2 as shown below:

$$\%R = \frac{C_o - C_e}{C_o} \times 100 \quad (1)$$

$$q_e = \frac{(C_o - C_e)V}{m} \quad (2)$$

With C_o and C_e indicating the initial and equilibrium phenol concentrations (mg/L), V and m denote the volume of phenol (L), and adsorbent mass (g) used respectively.

2.6 Kinetic Models

In this study, the linearized forms of intraparticle diffusion (ID), pseudo-first order (PFO), pseudo-second-order (PSO), and Elovich models were investigated to examine the kinetic data of phenol uptake onto ROP and ATOP.

The linear forms of the PFO and PSO models are given in equations 3 and 4 below [28-29]:

$$\ln(q_e - q_t) = \ln q_e - k_1 t \quad (3)$$

$$\frac{t}{q_t} = \frac{1}{k_2 q_e^2} + \frac{t}{q_e} \quad (4)$$

Where q_t represents the amount of phenol adsorbed at time t (min), k_1 and k_2 indicate the PFO and PSO rates constants (min^{-1}), and (g/mg min) respectively, and t is time in min.

The Elovich model is often used for heterogeneous solid surfaces and it is expressed in equation 5 as [28]:

$$q_t = \frac{1}{\beta}\ln(\alpha\beta) + \frac{1}{\beta}\ln t \quad (5)$$

Where α denotes the initial adsorption rate (mg g^{-1} min^{-1}), while the desorption constant is given as β (g mg^{-1}). The intraparticle diffusion model evaluates whether diffusion inside pores controls the sorption process. The linear form is expressed in equation 6 as [30]:

$$q_t = K_{id} t^{\frac{1}{2}} + C \quad (6)$$

K_{id} is the ID rate constant (mg g^{-1} $min^{1/2}$), and C is the boundary layer constant. The best kinetic fit was determined using the sum of squared errors (% SSE) in equation 7 [13]:

$$\%SSE = \frac{100}{N}\sqrt{\frac{(q_e - q_t)}{Q_e}}^2 \quad (7)$$

Where n denotes the number of data points.

2.7 Adsorption Isotherms

The mathematical models that explain the adsorbate interactions with adsorbents at equilibrium are referred to as adsorption isotherms. The Langmuir isotherm for instance, assumes that adsorption takes place in a single layer on a homogeneous surface with a limited number of identical sites, while on the other hand, the Freundlich model accounts for surfaces that are heterogeneous and allows for multilayer adsorption [3,15,31-32]. The mathematical linear expressions of Langmuir and Freundlich isotherms are represented in equations 8 and 9 below [31-32]:

$$\frac{C_e}{q_e} = \frac{C_e}{Q_{max}} + \frac{1}{Q_{max}K_L} \quad (8)$$

$$\log q_e = \log k_f + \left(\frac{1}{n}\right)\log C_e \quad (9)$$

$$R_L = \frac{1}{(1+bC_o)} \quad (10)$$

Equation 10 denotes the separation factor (R_L), which evaluates the feasibility of the Langmuir isotherm and is a dimensionless quantity [28, 31]. Where q_m and K_L stand for the maximum adsorption capacity (mg/g), and the Langmuir adsorption constant (L/mg), K_F and n are the Freundlich constant (mg/g), and dimensionless constant that denotes the adsorption intensity.

The Temkin isotherm proposed a decline in heat of adsorption with increasing coverage. The model can be expressed linearly as indicated in equation 11 [33]:

$$\ln q_e = \ln K_T + \frac{B}{R}\ln C_e \quad (11)$$

The Temkin isotherm constant that is associated with the adsorption energy is given as K_T (L/mg), the constant that associates with the heat of adsorption is denoted as B (J/mol), while R and T stand for the universal gas constant (8.314 J/mol·K), as well as the temperature (K).

Dubinin – Radushkevich (D-R) isotherm can be employed to differentiate between physical and chemical adsorption processes and the model can be illustrated linearly as shown in equation (12) [34]:

$$\ln q_e = lnq_o - K\varepsilon^2 \quad (12)$$

Where q_o is the calculated maximum adsorption capacity (mg/g), ε and K represent the Polanyi potential and the D-R constant that associates with the adsorption energy (mol^2/J^2). The mean free energy, E, that signifies the nature of the adsorption process, is expressed in equation 13 as [31-32]:

$$E = \frac{1}{\sqrt{2K}} \quad (13)$$

2.8 Thermodynamic parameters

Thermodynamic behavior was examined at various temperatures to evaluate parameters like Gibbs free energy change (ΔG), enthalpy change (ΔH), and entropy change (ΔS), using equations (14 and 15) [35-37]:

$$\Delta G^0 = -RT \ln K_D \quad (14)$$

$$\ln(\rho K_D) = -\frac{\Delta H}{RT} + \frac{\Delta S}{R} \quad (15)$$

Where K_D denotes the equilibrium constant (L/g), ρ is the water density (g/L) that was used to normalize the equilibrium constant and all other parameters are as previously defined.

3.0 Results and Discussions

3.1 *The influence of phenol concentration and contact time*

The influence of phenol concentrations as well as the contact time of the adsorption behavior of ROP and ATOP were examined and the obtained results are indicated in Figures 1 and 2 respectively. This was done by varying the initial phenol concentration between 50 to 300 mg/L and contact time between 5 to 300 min, while other parameters were kept constant. It was observed that the uptake of phenol increased with the contact time for both raw and acid-treated orange peel, and the rate of uptake was strongly influenced by the initial phenol concentration. A rapid increase in the amount adsorbed was observed within the first 50 min for both adsorbents, indicating abundant availability of vacant binding sites at the early stage [38-39]. As time progressed, the rate of uptake became slower and gradually approached equilibrium, where maximum uptake was observed at 150 min for ROP and ATOP. As the concentration increased to a point where the adsorbent was saturated, and no more active sites were accessible on the surface, the adsorption capacity of both adsorbents also increased, reaching their maximum uptake at 300 mg/L for both adsorbents [39]. For raw orange peel, the equilibrium uptake increased from 2.3–17.2 mg/g at 50 mg/L and from 18.5 –72.5 mg/g at 300 mg/L when the contact time rose from 5 to 150 min. For acid-treated orange peel, the uptake increased from 6.4–24.1 mg/g at 50 mg/L and from 25.6 –112.4 mg/g at 300 mg/L when the contact time rose from 5 to 150 min. The enhanced adsorption at higher concentrations suggests a stronger driving force for mass transfer from solution to the adsorbent surface [13].

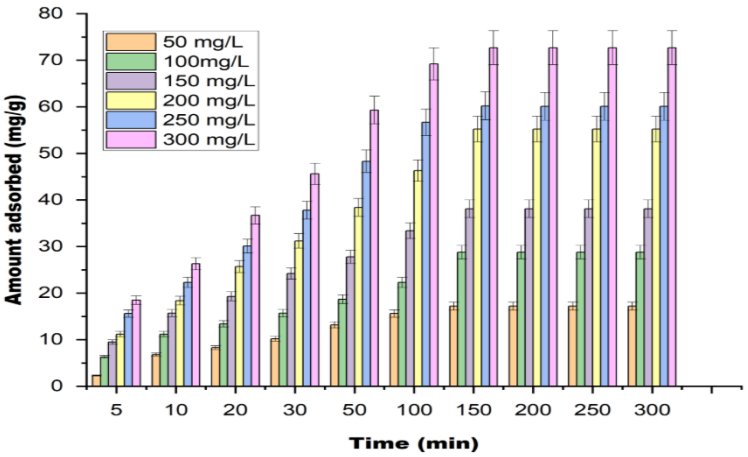

Fig. 1. Influence of phenol concentration and contact time on the sorption of phenol by raw orange peel

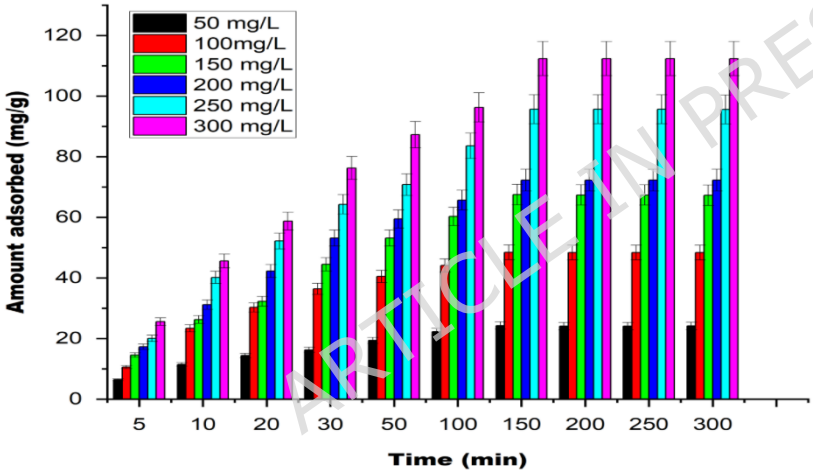

Fig. 2. Influence of phenol concentration and contact time on the sorption of phenol by acid-activated orange peel

3.2 *Influence of Orange Peel Dosage*

One of the substantial factors influencing the adsorption efficiency is the adsorbent dosage which is an important parameter. While other parameters were kept constant, the impact of the OP dosage was determined by varying the mass of the biomass between 5 to 40 mg. The removal percentage of phenol rose steadily with the adsorbent dosage for both ROP and ATOP (Fig. 3). At low dosages, removal efficiencies were low because of the presence of limited active surface area, but with a rise in the dosage, number of active sites as well as the available surface area increased proportionally,

resulting in greater phenol uptake. For ATOP, the maximum removal efficiency of 83.5 % was observed at 25 mg. ROP also followed a similar pattern, reaching its optimum at 20 mg with removal efficiency of 74.2 %. Beyond the optimum mass, no substantial improvement in removal was noticed for both adsorbents, and a slight decline appeared at higher dosages. This behaviour is linked to particle agglomeration at higher adsorbent dosage that reduces the effectiveness of the surface area and leads to overlapping of active sites [40]. Also, excessive adsorbent mass leads to a redistribution of phenol across a larger number of particles, lowering the apparent removal efficiency per unit mass. These observations are consistent with other findings, such as Jawad *et al* [40], who also observed a surge in the removal percentage of MB as the adsorbent dose increases.

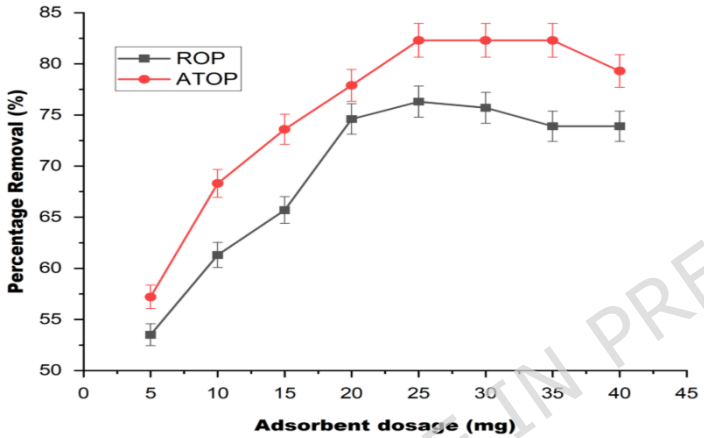

Fig. 3. Influence of OP dosage on the uptake of phenol by ROP and ATOP

3.3 *Influence of pH on phenol removal*

The solution's pH played a vital role in contaminant elimination process, influencing the adsorbent's surface chemistry and the extent to which the adsorbate ionized [3,15,40-41]. The point of zero charge (pH_pzc), which signifies the pH at which the surface of the adsorbent carries no net charge, was computed to be 4.7 for ROP and 3.5 for ATOP, reflecting the increased surface acidity induced by acid treatment [15, 40, 42]. At pH values smaller than the pH_pzc, particularly at pH 2, the surfaces of both adsorbents become strongly protonated due to the abundance of H^+ ions, causing reduced adsorption efficiency because of electrostatic repulsion and competition between phenol molecules and protons for available active sites [40, 42-43]. But with rise in the pH beyond the pH_pzc, surface deprotonation occurred, generating negatively charged functional groups that improved phenol uptake through stronger electrostatic interactions and hydrogen bonding [40, 42-43]. The impact of pH on the elimination of phenol using ROP and ATOP was examined at different pH values (2 to 10), while other parameters were kept constant. The efficiency of phenol removal was found to have surged as the pH was increased from acidic to basic medium (Fig. 4). Both raw and acid-activated orange peel showed their lowest removal efficiency at pH 2, where the adsorbent's surface was strongly protonated [3,15,40]. At this point, there is

competition between excess H^+ ions and phenol molecules, which leads to electrostatic repulsion and reduces adsorption efficiency [42]. As the pH increased, the removal efficiency also increased with ATOP surging from about 54.3 % at pH 2 to 80.1 % at pH 6, while ROP rose from 47.2 % to 76.3 % when the pH rose from 2 to 8. The higher removal efficiency at increased pH is because of the better electrostatic interaction between phenol and the available binding groups on the adsorbent surface, which is due to the deprotonation [43]. The maximum uptake for ATOP and ROP was attained at pH 6 and 8, respectively. At pH values greater than this for the maximum uptake, the removal efficiency began to decline gradually for both materials. This is because phenol partially dissociates at elevated pH, and the surface of adsorbent becomes more negatively charged, reducing attraction and lowering adsorption capacity [40].

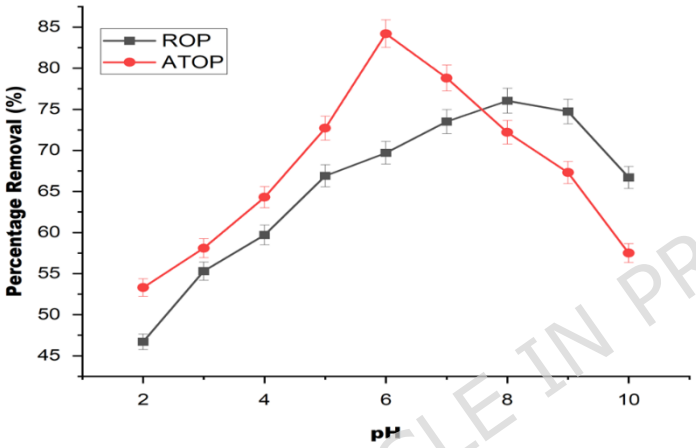

Fig. 4. Influence of pH on the uptake of phenol using ROP and ATOP

3.4 *Influence of temperature on phenol removal*

Temperature influence on the elimination of phenol using ATOP and ROP was evaluated over a range of 25 to 60 °C (Fig. 5) while keeping other variables constant. As reflected in Figure 5, as the temperature improved, the sorption efficiency also increased for both adsorbents. The rise in removal efficiency with temperature suggests enhanced mobility of phenol molecules and increased access to internal adsorption sites. The highest removal efficiency of 85.25 and 74.6% was attained at 50 °C for ATOP and 45 °C for ROP. Beyond the maximum temperature, the removal efficiency dropped for both adsorbents, which is because high temperature may disrupt the interaction between phenol molecules and surface functional groups, and also leads to partial desorption [43].

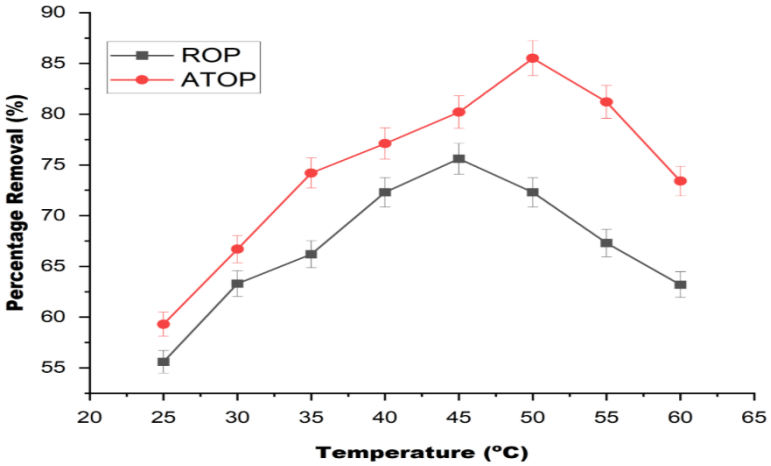

Fig. 5. Influence of temperature on the adsorption of phenol using ROP and ATOP

3.5 *Adsorption Kinetics*

The kinetic behaviour of phenol adsorption on ROP and ATOP surface was examined using PFO, PSO, Elovich, and ID models. The plots of these models are indicated in Figure 6, and the corresponding parameters are given in Tables 1 and 2 for ROP and ATOP, respectively. The results revealed different kinetic behaviors for the two adsorbents. The observed different kinetic behaviors for ROP and ATOP gave important insight into the adsorption pathway. For instance, the better fit of the pseudo-first-order model with data from ROP indicates that phenol removal is primarily governed by diffusion to relatively accessible surface sites with weak interaction energies. This kind of behavior is usually associated with adsorption dominated by physical interactions involving hydrogen bonding and van der Waals forces on comparatively uniform external surfaces [44]. Whereas, the kinetic data from ATOP are better described by the pseudo-second-order model which suggests that the overall rate is more strongly influenced by the availability of active sites and the strength of adsorbate–surface interactions involving chemisorption [40, 44]. The treatment of the adsorbent with an acid likely increased the density and heterogeneity of oxygen-containing functional groups (as observed from the EDS alaysis), creating sites with stronger specific interactions with phenol. The enhanced pore accessibility after activation also promotes faster intraparticle diffusion during the early adsorption stage, followed by site-controlled uptake at later times. Thus, the kinetic shift from ROP to ATOP reflects a transition from predominantly diffusion-limited physisorption to chemisorption.

The Elovich model also produced relatively good correlation for both adsorbents, showing that the adsorbents have a high affinity for phenol, with the initial sorption rate (α) higher than the desorption rate (β). The parameters also indicate that the surfaces are energetically heterogeneous. The intraparticle diffusion plots provide additional insight into the adsorption mechanism. For ROP, a lower intraparticle diffusion rate constant and a smaller intercept were observed, suggesting that surface adsorption is dominant, affirming the physisorption behavior of the adsorption process [35]. In

contrast, ATOP exhibits a higher intraparticle diffusion rate constant and a larger intercept, indicating a more pronounced influence of pore diffusion and boundary layer resistance. The multilinear nature of the plots for both adsorbents also confirms that it is not the sole rate-controlling step [29]. Therefore, acid activation significantly improved the adsorption kinetics, shifting the mechanism from a physisorption process in ROP to a chemisorption-driven process in ATOP.

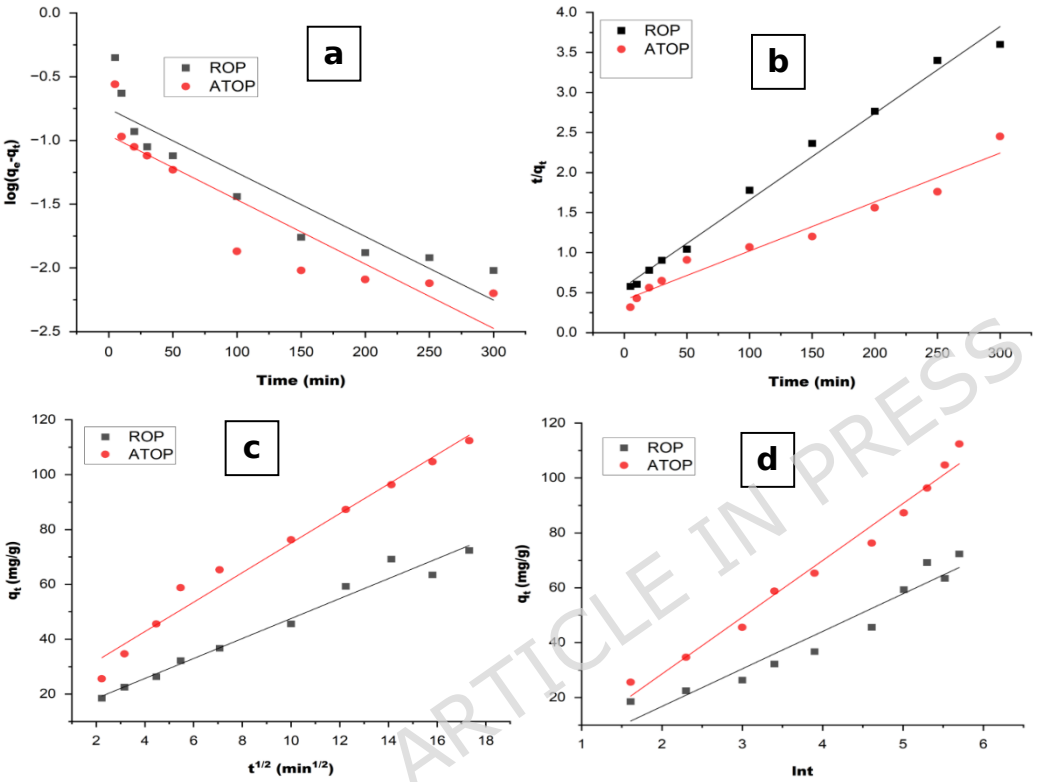

Fig. 6. (a) Pseudo first order, (b) Pseudo second order, (c) Intraparticle diffusion, (d) Elovich kinetics model for the elimination of phenols using ROP and ATOP

Table 1. Kinetic data for the elimination of phenol onto ROP

	First Order					Second order				Elovich			Intra-particle diffusion		
Ce	Q_e (exp)	Q_e (cal)	K_1	R^2	% SSE	Q_e (cal)	K_2	R^2	% SSE	α	β	R^2	K_p	C	R^2
22.3	17.200	18.09	0.037	0.988	0.016	23.92	0.168	0.927	0.118	2.952	0.176	0.956	1.648	0.375	0.994
45.8	28.800	26.66	0.041	0.966	0.022	35.76	0.142	0.946	0.073	3.629	0.297	0.956	3.717	0.664	0.974
76.3	38.100	40.08	0.062	0.994	0.016	42.36	0.322	0.933	0.034	4.282	0.451	0.942	5.264	0.894	0.989
97.3	55.200	58.04	0.068	0.997	0.016	66.97	0.291	0.927	0.064	7.081	0.698	0.997	7.074	1.273	0.984
112.34	60.200	61.81	0.071	0.996	0.008	81.55	0.184	0.933	0.107	7.795	0.714	0.977	9.345	5.107	0.995
145.3	72.700	74.42	0.093	0.995	0.007	92.32	0.746	0.921	0.081	9.045	0.749	0.992	11.189	5.942	0.994

Table 2. Kinetic data for the elimination of phenol onto ATOP

	First order					Second order				Elovich			Intra-particle diffusion		
C_e	Q_e (exp)	Q_e (cal)	K_1	R^2	% SSE	Q_e (cal)	K_2	R^2	% SSE	α	β	R^2	K_p	C	R^2
26.7	24.300	31.76	0.114	0.958	0.093	23.28	0.296	0.997	0.013	4.534	0.429	0.976	5.972	1.532	0.994
55.7	48.500	35.32	0.132	0.936	0.082	48.36	0.326	0.997	0.001	7.543	0.462	0.966	6.918	3.495	0.994
88.9	67.500	77.88	0.181	0.944	0.046	68.69	0.559	0.995	0.005	9.658	0.532	0.992	6.524	5.665	0.988
104.5	72.300	86.24	0.321	0.968	0.058	73.11	0.633	0.997	0.003	11.233	0.688	0.947	9.351	6.763	0.994
128.96	95.700	106.91	0.418	0.926	0.035	92.53	0.759	0.987	0.010	15.828	0.761	0.957	12.362	8.035	0.985
155.4	112.400	121.05	0.648	0.951	0.023	116.53	0.974	0.979	0.011	18.082	0.914	0.972	15.601	9.086	0.993

3.6 *Adsorption Isotherm*

The data obtained from equilibrium adsorption of phenol by ROP and ATOP were fitted to four different isotherm models as illustrated in Figure 7, and the corresponding variables are presented in Table 3. It can be observed that ROP best fits the Langmuir model, as signified by its high R^2 values. This indicates that phenol adsorption on the raw orange peel surface occurs predominantly on a homogeneous layer of active sites with uniform adsorption energies [31, 45]. In contrast, ATOP displayed a better fit with the Freundlich isotherm, evident from its high R^2 value and according to this model, adsorption takes place on a heterogeneous surface where the heat of adsorption varies across the adsorbent surface [32]. A reasonable maximum adsorption capacity (q_{max}) was deduced from the Langmuir model for both adsorbents, which is 80.32 mg g^{-1} for ROP, indicating a strong attraction between the phenol and the orange peel surface, and ATOP exhibiting higher value of 133.13 mg g^{-1} due to the modification of the adsorbent surface which has enhanced the functional groups present and improved its adsorption capacity.

Also, the value of the separation factor (R_L) obtained for both adsorbents is less than 1, which means the adsorption of phenol onto ROP and ATOP was favorable. The value of the Freundlich constant (n) obtained from the Freundlich model, which is also less than 1 for both adsorbents, affirms the favourability of the sorption process [46]. Table 4 presents a comparison of the q_{max} for both adsorbents with other low-cost adsorbents obtained from agricultural waste for phenol uptake. It can be deduced that the adsorption capacities of the adsorbent from these studies were competitive and can also be rated among existing adsorbents, which makes them a good candidate for sustainable phenol removal.

The improved performance of ATOP reflects the creation of a more heterogeneous surface after acid treatment, where phenol molecules interact through multilayer formation and a wider distribution of binding energies. The Temkin isotherm presumes the heat of adsorption decline linearly and proposes that sorption is characterized by a uniform spread of binding energies. The isotherm model of Dubinin-Radushkevich provides insight into biomass porosity and adsorption energy. The computed mean free adsorption energy (E) is 0.752 kJ/mol for ROP and 10.137 kJ/mol for ATOP. Literature suggests a free energy value below 8 kJ/mol typically indicates physisorption [47-48]. Therefore, the free energy computed indicates that the uptake process of ROP is controlled by physical adsorption, while ATOP is governed by chemical adsorption [47-48]. A recent study by Djama *et al*. [48], computed E values less than 8.0 kJ.mol^{-1} which confirmed the physical nature of the adsorption process of methylene blue.

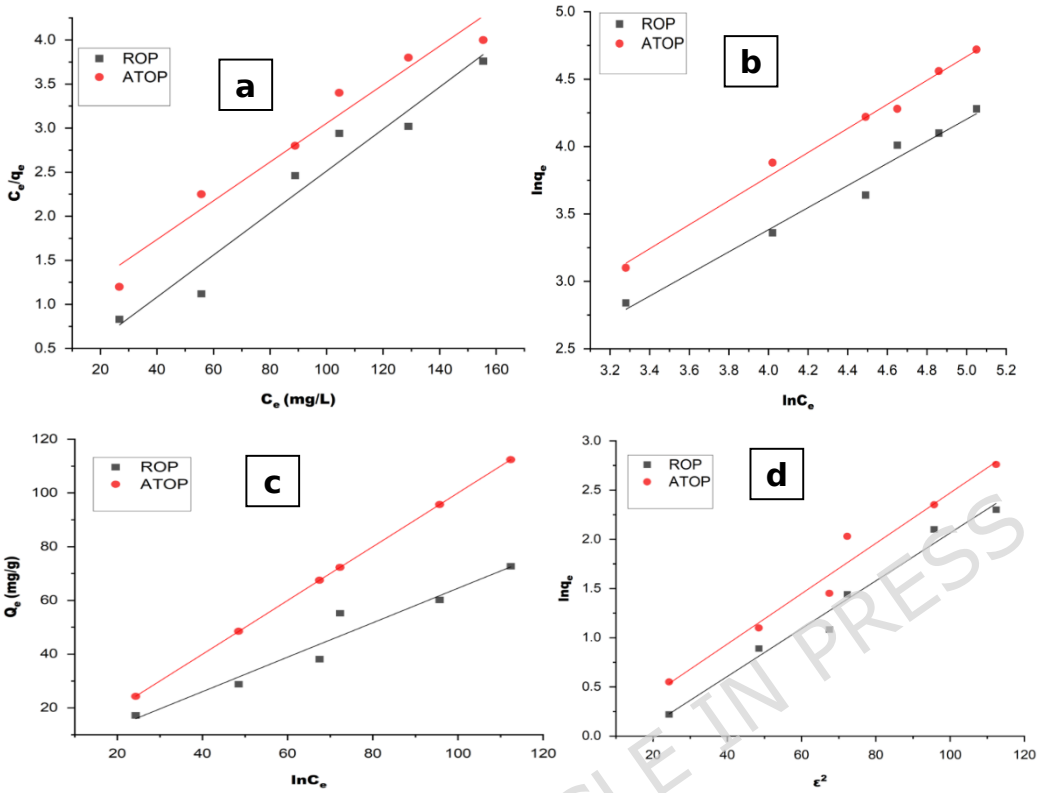

Fig. 7. Plots of: (a) Langmuir, (b) Freundlich, (c) Temkin, (d) Dubinin–Radushkevich isotherm model for the adsorption of phenol onto ROP and ATOP

Table 3. Parameters for phenol uptake by ROP and ATOP as obtained from the adsorption isotherm investigations

Isotherm	Parameters	ROP	ATOP
Langmuir	q_{max}	80.32	133.13
	R_L	0.221	0.23
	R^2	0.996	0.967
Freundlich	K_f	55.15	89.292
	1/n	0.605	0.512
	R^2	0.967	0.998
Temkin	A_T	0.265	0.867
	B_T	53.213	69.412
	R^2	0.955	0.955
Dubinin–Radushkevich (D-R)	Q_s	57.362	92.822
	E	0.752	10.137
	R^2	0.976	0.958

Table 4. Comparative analysis of the maximum adsorption capacities of ROP and ATOP for phenol uptake

Adsorbent	**Maximum adsorption capacities (q_{max}, mg/g)**	**Initial Dye Concentration**	**Adsorbent Dosage**	**pH**	**Temperature**	**Reference**
Cassia fistula pod	183.79	25 mg/L	1.6 g/L and 0.6 g/L	2.0	20°C	Patil *et al.* [3]
Shell activated carbon						
Natural clay	15	-	-	5.0	23°C	Djebbar *et al.* [42]
Sugarcane bagasse	159	100 ppm	-	4.0	25 °C	El-Bery *et al.* [49]
Black wattle bark	98.6	-	-	-	55 °C	Lütke *et al.* [50]
Cow dung	89.3	280 mg/L	0.6 g	6.5	45 °C	Ngueagni *et al.* [51]
Red clay brick	122.85, 137.46, and 152.22 mg/g	-	-	7.0	25°, 35°, and 45 °C	Abdel-Gawwad *et al.* [52]

ROP	80.32	300 mg/L	20 mg	8.0	50 °C	This study
ATOP	133.13	300 mg/L	25 mg	6.0	45 °C	This study

3.7 *Thermodynamic Studies*

The spontaneity and nature of phenol on ROP and ATOP were determined from the plots shown in Figure 8, and their values as indicated in Table 5. For both adsorbents, the Gibbs free energy values (ΔG) were negative within the studied temperature range, confirming the uptake process to be spontaneous [35,40,43,45]. The positive enthalpy change (ΔH°) for both adsorbents signifies that phenol uptake is endothermic, inferring that higher temperatures enhance uptake [43]. This behavior is commonly associated with enhanced mobility of phenol molecules and increased penetration into microporous structures. The more pronounced value observed for ATOP implies that acid treatment increases the active surface sites and pore structure, leading to stronger interaction between the adsorbent surface and phenol molecules [53]. In addition, the ΔH value can indicate the nature of the adsorption process, with values between 1-40 kJ/mol typically fall into the physisorption range [35,40,43,45]. For ROP, the ΔH° value found was 14.5 kJ/mol, which implies that the sorption process is governed by physisorption, whereas the ΔH° value for ATOP is evaluated to be 45.32 kJ/mol, signifying the uptake process to be chemisorption [54]. The positive entropy values reflect improved disorder at the solid–liquid interface during adsorption. The higher ΔS for ATOP suggests greater structural rearrangement and better diffusion of phenol molecules into the activated sites. This increase in entropy may arise from the displacement of structured water molecules from the adsorbent surface and phenol hydration shell, which contributes favorably to the overall adsorption driving force.

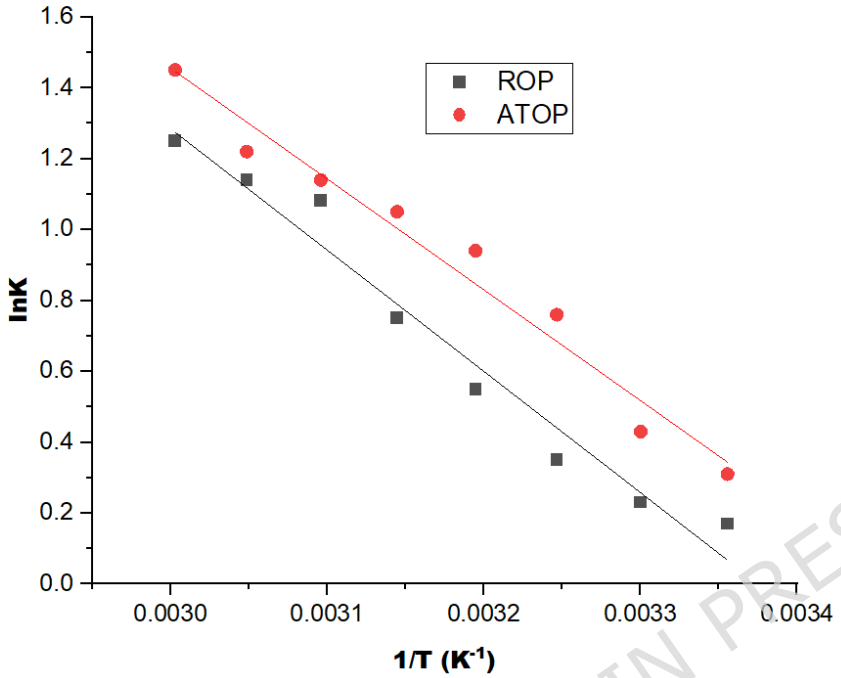

Fig. 8. Thermodynamics plot for the adsorption of phenol onto ROP and ATOP

Table 5. Parameters obtained for the thermodynamic analysis of the sorption of phenol by ROP and ATOP

	ROP			ATOP		
T (K)	ΔG (kJ/mol)	ΔH (kJ/mol)	ΔS (kJ/mol)	ΔG (kJ/mol)	ΔH (kJ/mol)	ΔS (kJ/mol)
298	-0.62			-3.07		
303	-1.05			-7.26		
308	-2.75			-9.21		
313	-3.56	14.5	5.7×10^{-2}	-13.24	45.32	1.9×10^{-1}
318	-6.43			-16.21		
323	-8.06			-19.35		
328	-10.23			-22.03		
333	-12.25			-25.03		

3.8. Adsorbent Structural Elucidation with Different Analytical Tools

The SEM micrographs shown in Figure 9 clearly indicated morphological changes on the orange peel surface before and after phenol sorption. The raw peel (a) exhibits a

highly fibrous, irregular, and porous structure with open cavities, elongated fibers, and cracks; a morphology, which is often associated with citrus peels and other agro-waste adsorbents [55]. After contact with phenol (b), the biomass surface becomes partially covered and more compact. The visible pores or cavities initially seen appear to be coated or filled and flake-like deposits or smoother patches appear on the fibres. This kind of surface coverage and pore-filling after organic contaminant sorption have been observed in orange-peel derived adsorbents, is consistent with successful surface sorption or adsorbate precipitation on the surface of the adsorbent [56].

The FT-IR investigation of orange peel prior and after adsorption of phenol is illustrated in Figure 10. The broad band seen around 3250–3675 cm^{-1} is assigned to –OH stretching vibrations from hydroxyl groups in cellulose, hemicellulose, lignin, and pectin, as well as adsorbed water [45,57-59]. The band noticed at 2950 cm^{-1} is due to C–H band, while the band observed at 1734 cm^{-1} is associated with C=O band of ester and carboxylic groups, mainly from pectin [55-56]. The bands seen between 1620–1633 cm^{-1} can be attributed to aromatic C=C stretching [57, 60], while bands in the range 1230–1040 cm^{-1} are due to C–O and C–O–C vibrations of polysaccharides [45,57-59].

After the sorption of phenol, noticeable changes were seen in the FTIR spectrum. The –OH stretching band (3250 cm^{-1}) becomes less intense and slightly shifted to 3335–3688 cm^{-1}, suggesting the participation of hydroxyl groups in hydrogen bonding with phenol molecules. The C=O band near 1725 cm^{-1} shows a decline in intensity or slight shift to 1745 cm^{-1}, signifying interaction between ester/ carboxyl groups on the orange peel surface and phenol. Only slight peak modification was seen around 1615 cm^{-1} which can be attributed to aromatic ring vibrations of phenol, confirming its presence on the surface of the adsorbent. Furthermore, alteration in the 1205–1012 cm^{-1} region infers the contribution of C–O functional groups during adsorption.
In all, the shifts in intensity, and appearance of additional bands in spectrum (b) compared to (a) signify that phenol adsorption onto orange peel occurs mainly through hydrogen bonding, and possible electrostatic interactions involving hydroxyl, carboxyl, and aromatic functional groups. These FTIR results support the successful adsorption of phenol and corroborate the SEM observations of surface modification after adsorption

The cumulative pore volume and pore size distribution results show that acid-treated orange peel possesses a predominantly microporous structure, with pore diameters observed within the range of 0.15–0.6 nm (Fig. 11). A pronounced rise in both the cumulative pore volume and differential pore volume within 0.28–0.35 nm signify that most pores are concentrated within this narrow micropore region [59, 61]. This characteristic reflects the effectiveness of acid modification in removing inorganic impurities and unstable organic components, thus opening earlier blocked pores and generating new ultramicropores. The cumulative pore volume rises smoothly with pore diameter, attaining about 22–23 cc g^{-1}, which signify a well-developed and

interconnected pore network instead of isolated pores. The presence of slightly wider micropores likely enhances diffusion into smaller pores, enabling accessibility. In all, the developed microporosity and increased pore volume show that acid-treated orange peel is structurally well suited for adsorption applications, most especially for the elimination of heavy metals, dyes, and small organic contaminants. Acid-activated orange peel biomass has been reported to develop enhanced pore structure and adsorption capacity, as exhibited in methylene blue removal studies using H_2SO_4 activation and in metformin adsorption using H_3PO_4 activation, with N_2 adsorption (BET) used to examine the pore development [62].

The XRD patterns of orange peel before and after phenol uptake (Fig. 12) demonstrated a broad diffraction hump centered around $2\theta \approx 18–25°$, which is a feature of amorphous lignocellulosic materials such as cellulose, hemicellulose, lignin, and pectin [55,59**]**. The broad peak seen near $2\theta \approx 22°$ corresponds to the (002) plane of cellulose I, signifying the presence of semi-crystalline cellulose domains embedded within an amorphous matrix [55,60]. The absence of sharp diffraction peaks affirms the predominantly amorphous nature of the biomass [55,57]. After phenol uptake, no new crystalline phases were observed suggesting that the uptake process did not alter the fundamental structure of the biomass [56,59]. A slight reduction in peak intensity and increased peak broadening were seen, indicating surface coverage and partial disruption of ordered regions because of phenol deposition [56,61]. The absence of additional diffraction peaks further affirms that phenol molecules were adsorbed onto the surface without crystallization [59,62], supporting adsorption dominated by surface interactions rather than bulk structural modification [55,56,62].

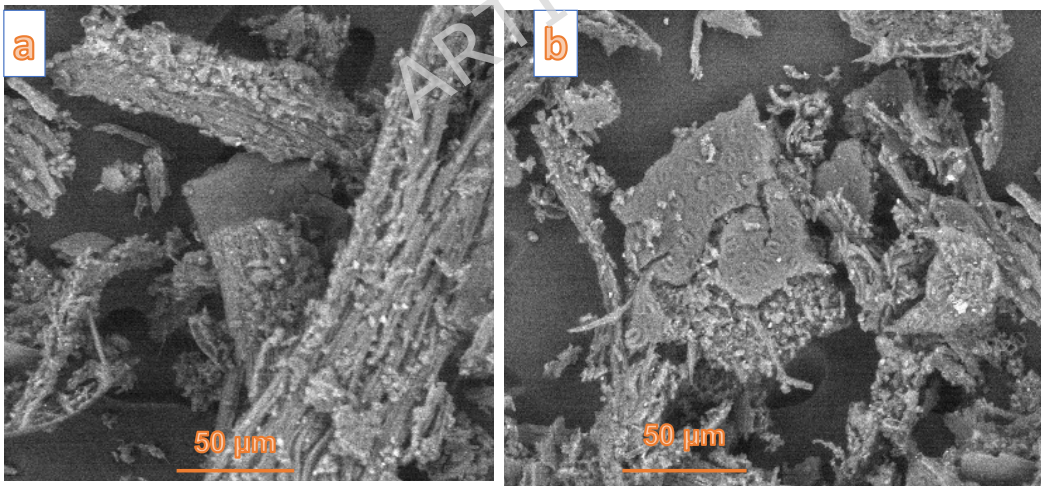

Fig. 9: SEM images of acid-activated orange peel (a) before and (b) after phenol adsorption

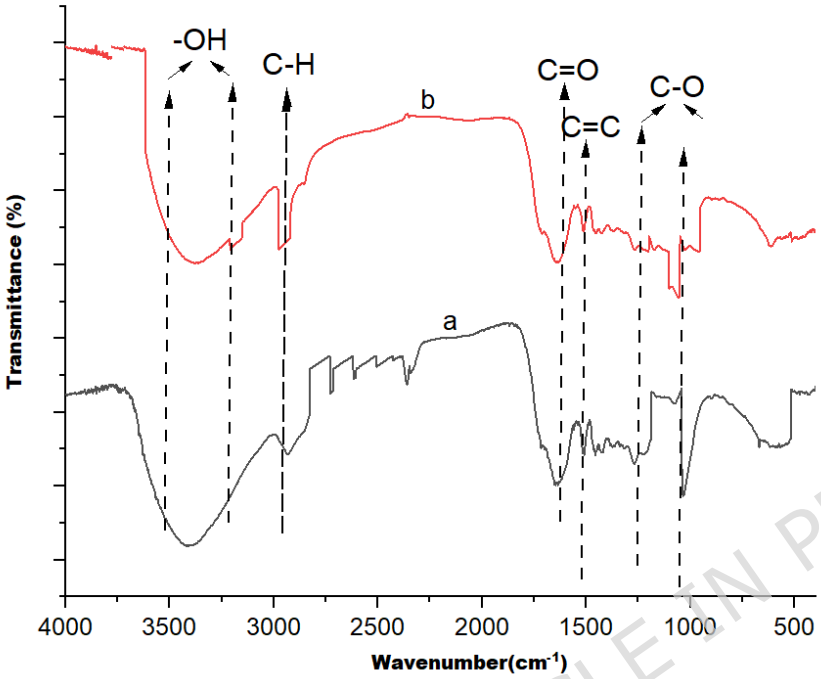

Fig. 10: FTIR structural evolution of acid-activated orange peel (a) before and (b) after phenol adsorption

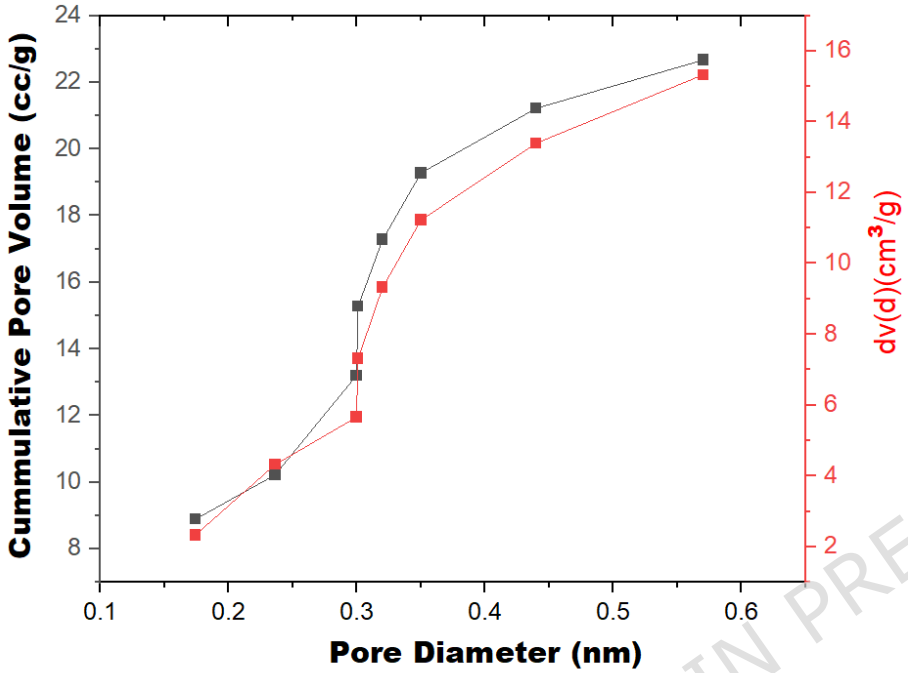

Fig. 11: Pore Size Distribution and Cumulative Pore Volume of Acid-Treated Orange Peel Adsorbent

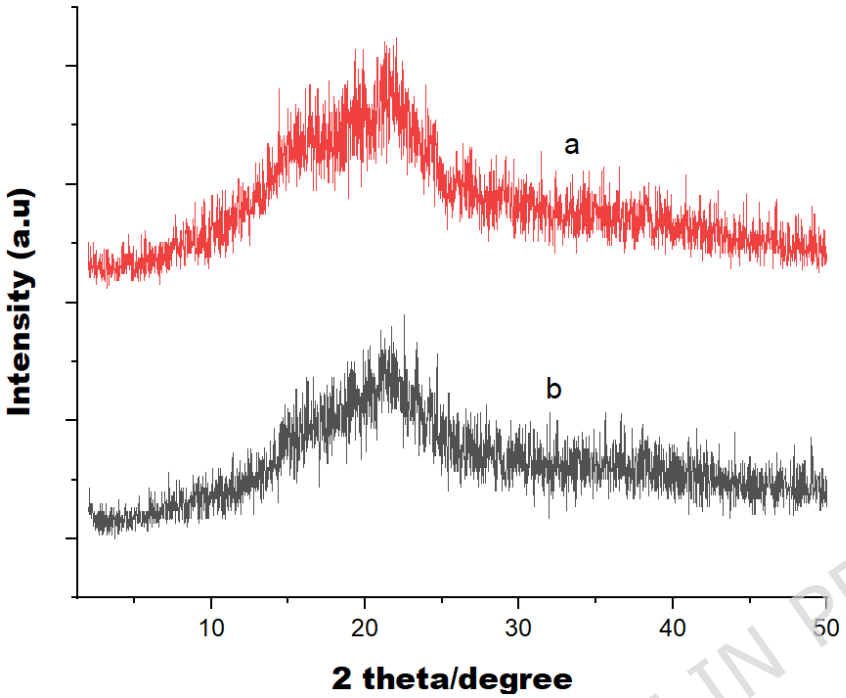

Fig. 12: XRD of acid-activated orange peel (a) before and (b) after phenol adsorption

3.9 *Mechanism of Adsorption*

The mechanism of the uptake of phenol onto orange peel–derived adsorbents is governed by the surface chemistry and pore structure of the lignocellulosic matrix. As evidenced by the combined physicochemical characterization and adsorption modeling, the adsorption mechanism involves multiple interactions whose relative contributions differ between ROP and ATOP. First, findings from the pH_pzc results indicate the electrostatic environment. The treatment of the peel with an acid increases the surface acidity due to the lowered pH_pzc, and promoting the formation of negatively charged sites at near-neutral pH. The enhanced surface polarity of ATOP eases stronger dipole–dipole and specific interactions compared with ROP, even though phenol is largely molecular in the studied pH range. Based on the findings from FTIR analysis, abundance of functional groups corresponding to hydroxyl (–OH), carboxyl (–COOH), and aromatic inherent to cellulose, hemicellulose, lignin, and pectin were identified. After the uptake of phenol, the weakening and shifting of the –OH stretching band together with changes in the C=O region observed signify the likely involvement

of hydroxyl and carboxyl groups in hydrogen bonding with phenol molecules. These interactions are expected since phenol possesses a polar hydroxyl group that can act as both hydrogen bond donor and acceptor.

BET and pore size distribution analyses validate that acid activation may have opened previously blocked pores and generated ultramicroporous structures which enhances pore diffusion and confinement effects, permitting the molecules of phenol to access internal binding sites more effectively. This is corroborated from SEM investigation which shows pore filling after adsorption supporting the pore-occupation mechanism.

Furthermore, reports from kinetic and isotherm modeling suggested additional mechanistic insight. For instance, the pseudo-second-order kinetics and Freundlich behavior of ATOP signify adsorption on energetically heterogeneous sites involving stronger surface interactions. In contrast, the pseudo-first-order and Langmuir behavior of ROP indicate adsorption dominated by relatively weak surface interactions on energetically uniform sites, which is made up of physisorption controlled by hydrogen bonding and van der Waals forces. Finally, the moderate enthalpy change for ROP signify physical adsorption, however the higher value for ATOP indicates the participation of stronger specific interactions after acid activation. The schematic representation of the mechanism of sorption for the removal of phenol onto ROP and ATOP is shown in Figure 13.

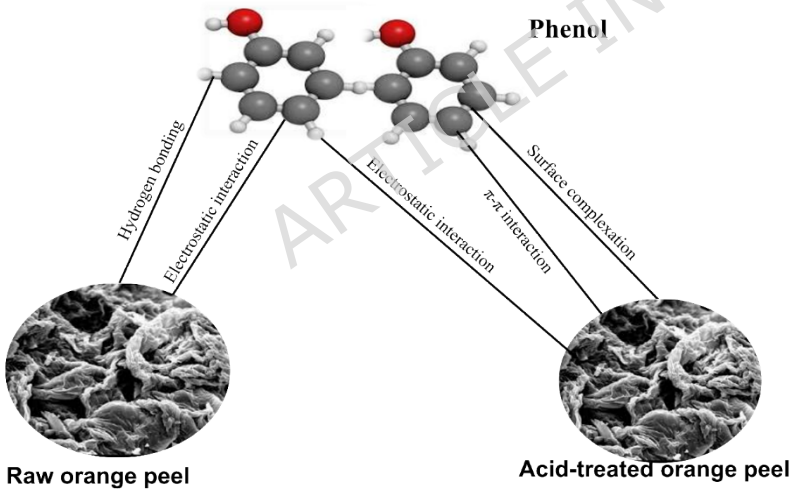

Fig. 13. Adsorption mechanism for the removal of phenol onto ROP and ATOP

Table 6. Performance of acid-activated biomass adsorbents comparison of phenol adsorption

Adsorbent	Activation approach	Processing condition	q_{max} (mg g^{-1})	Isotherm model	Reference
Orange peel activated char (KOH + pyrolysis)	KOH + 800 °C	Two-step carbonization	360–467	Langmuir/Freundlich	Kumar et al. [63]
Mixed agro-waste activated carbon	Chemical activation	Conventional AC	8.27	Langmuir	Monica et al. [64]
Orange peel biochar (thermal only)	Pyrolysis (300–700 °C)	-	31 (at 700 °C)	—	Kumar et al. [65]
Wheat straw biochar (acid-washed + CO_2 activated)	HF wash + 900 °C CO_2 activation	High-temperature activation	471.16	Langmuir	Zhou et al. [66]
Acid-treated orange peel	HCl (mild)	No carbonization	133.13	Freundlich	This study

The adsorption performance of the adsorbent from this study relative to other acid-activated biomass adsorbents reported in the literature was further investigated as illustrated in Table 6. The comparison shows three vital points. First, highly activated carbons which was formed via strong chemical activation and high-temperature pyrolysis (≥800–900 °C) shows high adsorption capacities (>350 mg g^{-1}) because of their extremely developed surface areas and aromatic carbon structures [63]. Also, non-activated biomass or low-temperature materials generally show much lower capacities (<50 mg g^{-1}), indicating the importance of surface modification in enhancing phenol uptake [65]. Finally, the HCl-modified orange peel developed in this study achieves

competitive adsorption capacity (133.13 mg g^{-1}) using a mild, low-energy treatment without carbonization, placing it in an advantageous middle ground between raw biosorbents and energy-intensive activated carbons. This highlights its potential as a cost-effective and scalable alternative for phenolic wastewater treatment where process simplicity and sustainability are prioritized.

3.10 Implications and Limitations of the Study

The potential of agro-waste activation in sustainable wastewater treatment was highlighted based on findings in this study which reveal that acid-treated orange peel waste can serve as low-cost, efficient, and environmentally benign adsorbent for phenol elimination. The transformation of an abundant agricultural waste into a high-performance adsorbent is in alignment with the principles of circular economy through the reduction of waste generation and providing a value-added material for the remediation of the environment. The improvement in adsorption capacity as observed and the shift in mechanism toward chemisorption further indicate that tailoring biomass-derived adsorbents for specific contaminants can be achieved through controlled surface modification which is an effective strategy. Notwithstanding these promising findings, certain limitations are to be acknowledged. First, sorption studies were performed under batch conditions using simulated phenol solutions, which may not fully signify the complexity of real wastewater from the industrial containing co-contaminants and competing ions. Furthermore, regeneration and reuse of the adsorbent were not conducted in this study, which is critical for large-scale and economic feasibility. The structural stability of acid-treated orange peel under repeated adsorption–desorption cycles in a long-term exposure also remains to be evaluated. Therefore, future works should focus on adsorbent column-scale or continuous-flow, and regeneration experiments, and conduct assessment in real wastewater systems. These kinds of experiments would provide deeper understanding into the scalability and practical applicability of acid-treated orange peel for industrial wastewater treatment.

4.0 Conclusion

In this work, orange peel biomass was effectively modified with mild HCl treatment to improve its performance for the removal of phenol from aqueous solution. The combination of physicochemical characterization and adsorption modeling showed that acid activation improved the surface acidity, pore accessibility, and generates a more heterogeneous distribution of active sites. These surface alterations via acid treatments shift the adsorption pathway toward stronger and more diverse phenol–surface interactions while maintaining the low-cost and sustainable nature of the precursor material. The favorable thermodynamic behavior and competitive adsorption capacity of acid-treated orange peel biomass showcased it as a substitute to conventional adsorbents, particularly for usage where sustainability, cost, and material accessibility are critical considerations. The results support the potential of acid-treated orange peel as a promising adsorbent for phenolic wastewater treatment.

Declarations

Conflict of interest:

No conflict of interest exists.

Ethical approval: N/A

Acknowledgments:

Princess Nourah bint Abdulrahman University Researchers Supporting Project number (PNURSP2026R13), Princess Nourah bint Abdulrahman University, Riyadh, Saudi Arabia.

Data Availability: The datasets used and/or analysed during the current study available from the corresponding author on reasonable request.

Authors Contributions: Zahrah Alqahtani carried out the characterizations and statistical analysis, Oladejo Emmanuel Kola conceived the work, and performed the experiments, Aliyah Alsharif read the first draft and performed statistical analysis, Ali Shawabkeh and Afnan M. Alnajeebi provide resources, and performed data analysis, Roaa A.Tayeb performed statistical analysis and contributed resources, Amani Fahm Mohammed Al Solami and Hamad AlMohamadi performed data analysis, contributed in characterization, and contributed resources, Jamelah S. Al-Otaibi contributed financial assistance, performed statistical analysis, and resources.

Funding:

This work was funded by Princess Nourah bint Abdulrahman University Researchers Supporting Project number (PNURSP2026R13), Princess Nourah bint Abdulrahman University, Riyadh, Saudi Arabia.

References

[1] Ahmaruzzaman M, Mishra SR, Gadore V, *et al*. Phenolic compounds in water: From toxicity and source to sustainable solutions – An integrated review of removal methods, advanced technologies, cost analysis, and future prospects. J Environ Chem Eng. 2024;12(3):112964. doi:10.1016/j.jece.2024.112964

[2] Mohd A. Presence of phenol in wastewater effluent and its removal: An overview. Int J Environ Anal Chem. 2022;102(6):1362–1384. doi:10.1080/03067319.2020.1738412

[3] Patil P, Jeppu G, Vallabha MS, Girish CR. Enhanced adsorption of phenolic compounds using biomass-derived high surface area activated carbon: Isotherms, kinetics and thermodynamics. Environ Sci Pollut Res. 2024. doi:10.1007/s11356-024-32971-1

[4] Pavithra KG, Sundar Rajan P, Arun J, Brindhadevi K, Le QH, Pugazhendhi A. A review on recent advancements in extraction, removal and recovery of phenols from phenolic wastewater: Challenges and future outlook. Environ Res. 2023;237:117005. doi:10.1016/j.envres.2023.117005

[5] Sun J, Mu Q, Kimura H, *et al*. Oxidative degradation of phenols and substituted phenols in the water and atmosphere: A review. Adv Compos Hybrid Mater. 2022;5:627–640. doi:10.1007/s42114-022-00435-0

[6] Mainali K. Phenolic compounds contaminants in water: a Glance. CTCSE. 2020;4(4):1–3. doi:10.33552/CTCSE.2020.04.000593

[7] Khan MN, Siddique M, Mirza N, *et al*. Synthesis, characterization, and application of Ag-biochar composite for sono-adsorption of phenol. Front Environ Sci. 2022;10:823656. doi:10.3389/fenvs.2022.823656

[8] Njimou JR, Godwin J, Pahimi H, *et al*. Biocomposite spheres based on aluminum oxide dispersed with orange-peel powder for adsorption of phenol from batch membrane fraction of olive mill wastewater. Colloid Interface Sci Commun. 2021;42:100402. doi:10.1016/j.colcom.2021.100402

[9] Pavithra KG, Sundar Rajan P, Arun J, Brindhadevi K, Le Hoang Q, Pugazhendhi A. A review on recent advancements in extraction, removal and recovery of phenols from phenolic wastewater: Challenges and future outlook. Environ Res. 2023;237:117005. doi:10.1016/j.envres.2023.117005

[10] Mamman S, Abdullahi SS, Birniwa AH, *et al*. Influence of adsorption parameters on phenolic compounds removal from aqueous solutions: A mini review. Desalin Water Treat. 2024;320:100631. doi:10.1016/j.dwt.2024.100631

[11] Ayach J, El Malti W, Duma L, *et al*. Comparing Conventional and Advanced Approaches for Heavy Metal Removal in Wastewater Treatment: An In-Depth Review Emphasizing Filter-Based Strategies. Polymers. 2024;16:1959. doi:10.3390/polym16141959

[12] Ofudje EA, Sodiya EF, Akinwunmi F, Ogundiran AA, Oladeji OB, Osideko OA. Eggshell derived calcium oxide nanoparticles for Toluidine blue removal. Desalin Water Treat. 2022;247:294-308. doi:10.5004/dwt.2022.28079

[13] Haydari I, Aziz K, Elleuch J, *et al*. Synergistic strategies for phenol removal from olive mill wastewater (OMWW): a combined experimental and theoretical investigation using Chlorococcum sp.-derived CuO nanoparticles. Biomass Bioenergy. 2025;192:107483. doi:10.1016/j.biombioe.2024.107483.

[14]. Guediri, A., Bouguettoucha, A., Tahraoui, H. et al. Thermodynamic study and the development of a support vector machine model for predicting adsorption behavior of orange peel-derived beads in wastewater treatment. Journal of

Molecular Liquids, 403, 124860. https://doi.org/10.1016/j.molliq.2024.124860 (2024).

[15] Singh D. Insights into Adsorbents: Activated Carbon for Effective Adsorption. Jabirian J Biointerface Res Pharm Appl Chem. 2024;1:11–21. doi:10.55559/jabirian.v1i02.233

[16] Ullah S, Shah SSA, Altaf M, *et al*. Activated carbon derived from biomass for wastewater treatment: Synthesis, application and future challenges. J Anal Appl Pyrolysis. 2024;179:106480. doi:10.1016/j.jaap.2024.106480

[17]. Reffas, A., Bouguettoucha, A., Chebli, D. et al. Adsorption of ethyl violet dye in aqueous solution by forest wastes, wild carob. *Desalination and Water Treatment*, *57*(21), 9859–9870. https://doi.org/10.1080/19443994.2015.1031707 (2016).

[18]. Bouguettoucha, A., Reffas, A., Chebli, D. et al. Novel activated carbon prepared from an agricultural waste, *Stipa tenacissima*, based on $ZnCl_2$ activation—characterization and application to the removal of methylene blue. *Desalination and Water Treatment*, *57*(50), 24056–24069. https://doi.org/10.1080/19443994.2015.1137231 (2016).

[19] Iheanacho OC, Nwabanne JT, Obi CC, Onu CE. Packed bed column adsorption of phenol onto corn cob activated carbon: Linear and nonlinear kinetics modeling. South Afr J Chem Eng. 2021;36:80–93. doi:10.1016/j.sajce.2021.02.003

[20] Singh R, Dutta RK, Naik DV, Ray A, Kanaujia PK. High surface area Eucalyptus wood biochar for the removal of phenol from petroleum refinery wastewater. Environ Challenges. 2021;5:100353. doi:10.1016/j.envc.2021.100353

[21] Elayadi F, Boumya W, Achak M, *et al*. Experimental and modeling studies of the removal of phenolic compounds from olive mill wastewater by adsorption on sugarcane bagasse. Environ Challenges. 2021;4:100184. doi:10.1016/j.envc.2021.100184

[22] Bhatia D, Saroha AK. Biochar derived from pyrolysis of rice straw as an adsorbent for removal of phenol from water. J Water Process Eng. 2024;59:105003. doi:10.1016/j.jwpe.2024.105003.

[23]. Michael-Igolima, U., Abbey, S. J., Ifelebuegu, A. O. et al. Modified orange peel waste as a sustainable material for adsorption of contaminants. *Materials*, *16*(3), 1092. https://doi.org/10.3390/ma16031092 (2023).

[24]. Andriambahiny, R.N.A., Das, J., Roy, B. *et al.* A review on the recent advancement of acid modified bio-adsorbents for the removal of methyl orange dye from wastewater treatment. *Discov. Chem.* 2, 92. https://doi.org/10.1007/s44371-025-00180-5 (2025).

[25]. Tang, K. H. D. Valorization of organic waste as biosorbents for wastewater treatment. *Water Emerg. Contam. Nanoplastics 3*, 25. http://dx.doi.org/10.20517/wecn.2024.53 (2024).

[26]. Kalengyo, R.B., Ibrahim, M.G., Fujii, M. *et al.* Utilizing orange peel waste biomass in textile wastewater treatment and its recyclability for dual biogas and biochar production: a techno-economic sustainable approach. *Biomass Conv. Bioref.* 14, 19875–19888. https://doi.org/10.1007/s13399-023-04111-1 (2024).

[27]. Kumar, L., Hakeem, I.G., Varathan, E. *et al.* Adsorption of Phenol from Aqueous Solution using Activated Char Synthesized by One-Step and Two-Step KOH Activation and Pyrolysis of Orange Peel. *Water Air Soil Pollut* 236. https://doi.org/10.1007/s11270-025-08431-y 803 (2025).

[28] Mesquita MDS, Tanabe EH, Bertuol DA. Adsorption of phenol using Eucalyptus saligna biochar activated with NiCl$_{2}$. Water Air Soil Pollut. 2024;235(5):Article 311. doi:10.1007/s11270-024-07049-w

[29] Ezzati R, Azizi M, Ezzati S. A theoretical approach for evaluating the contributions of pseudo-first-order and pseudo-second-order kinetics models in the Langmuir rate equation. Vacuum. 2024;222:113018. doi:10.1016/j.vacuum.2023.113018

[30] Guo X, Wang J. A novel monolayer adsorption kinetic model based on adsorbates “infect” adsorbents inspired by epidemiological model. Water Res. 2024;253:121313. doi:10.1016/j.watres.2024.121313

[31] Din SU, Ofudje EA, Al-Ahmary KM, *et al*. Sorghum husks as potential low cost adsorbent for Congo red adsorption. Sci Rep. 2025;15(1):38265. doi:10.1038/s41598-025-22082-3

[32] Fito J, Abewaa M, Mengistu A, *et al*. Adsorption of methylene blue from textile industrial wastewater using activated carbon developed from Rumex abyssinicus plant. Sci Rep. 2023;13:5427. doi:10.1038/s41598-023-32431-8

[33] Nafisyah E, Arrisujaya D, Susanti E. The utilization of water hyacinth (Eichhornia crassipes) harvested from the phytoremediation process as activated carbon in Cr(VI) adsorption. *IOP Conf Ser Earth Environ Sci*. 1211:012019. doi:10.1088/1755-1315/1211/1/012019 (2023).

[34] Ananpreechakorn W, Seetawan T. Synthesis and Characterization of Activated Carbon from Water Hyacinth. J Phys Conf Ser. 2013:012025. doi:10.1088/1742-6596/2013/1/012025 (2021).

[35] Ghosh N, Sen S, Biswas G, Saxena A, Haldar PK. Adsorption and desorption study of reusable magnetic iron oxide nanoparticles modified with justicia adhatoda leaf extract for the removal of textile dye and antibiotic. Water Air Soil Pollut. 234(3):202. doi:10.1007/s11270-023-06217-8 (2023).

[36]. Chebli, D., Bouguettoucha, A., Mekhalef, T. et al. Valorization of an agricultural waste, *Stipa tenassicima* fibers, by biosorption of an anionic azo dye, Congo red. *Desalination and Water Treatment* 54, 245–254. doi: 10.1080/19443994.2014.880154 (2015).

[37]. Bouguettoucha, A., Chebli, D., Mekhalef, T. et al. The use of a forest waste biomass, cone of *Pinus brutia* for the removal of an anionic azo dye Congo red from aqueous medium. *Desalination and Water Treatment* 55, 1956–1965. doi: 10.1080/19443994.2014.928235 (2015).

[38] Kori AK, Ramavandi B, Mahmoodi SMM, Javanmardi F. Magnetization and ZIF-67 modification of Aspergillus flavus biomass for tetracycline removal from aqueous solutions: a stable and efficient composite. Environ Res. 2024;252(Pt 2):118931. doi:10.1016/j.envres.2024.118931

[39] Chikri R, Elhadiri N, Benchanaa M, Maguana Y. Efficiency of sawdust as low-cost adsorbent for dyes removal. J Chem. 2020:1–17. doi:10.1155/2020/6902409

[40] Jawad AH, Abdulhameed AS, Mastuli MS. Acid-factionalized biomass material for methylene blue dye removal: a comprehensive adsorption and mechanism study. J Taibah Univ Sci. 2020;14(1):305–313. doi:10.1080/16583655.2020.1736767

[41] Oyetade JA, Machunda RL, Hilonga A. Fenton-mediated solar-driven photocatalysis of industrial dye effluent with polyaniline impregnated with activated TiO_2-Nps. J Photochem Photobiol A. 2024;20:100231. doi:10.1016/j.jpap.2024.100231

[42] Djebbar M, Djafri F, Bouchekara M, Djafri A. Adsorption of phenol on natural clay. Appl Water Sci. 2012;2(2):77–86. doi:10.1007/s13201-012-0031-8

[43] Sarici-Ozdemir Ç, Kiliç F. Kinetics behavior of methylene blue onto agricultural waste. Part Sci Technol. 2018;36(2):194–201. doi:10.1080/02726351.2016.1240127

[44] Albert AA, Chenping G, Runping H, Lingbo Q. Functionalized magnetic biocomposite based on peanut husk for the efficient sequestration of basic dyes in single and binary systems: adsorption mechanism and antibacterial study. J Environ Chem Eng. 2022;10(4):108205. doi:10.1016/j.jece.2022.108205

[45] Ogundiran, A. A., Ofudje, E. A., Ogundiran, O. O., and Adewusi, A. M. (2022). “Cationic dye adsorptions by eggshell waste: Kinetics, isotherms and thermodynamics studies,” Desalination & Water Treatment 280, 157-167. DOI: 10.5004/dwt.2022.29080

[46] Somsesta N, Sricharoenchaikul V, Aht-Ong D. Adsorption removal of methylene blue onto activated carbon/cellulose biocomposite films: equilibrium and kinetic studies. Mater Chem Phys. 2020;240:122221. doi:10.1016/j.matchemphys.2019.122221

[47] Damahe D, Mayilswamy N, Kandasubramanian B. Biochar/metal nanoparticles-based composites for dye remediation: a review. Hybrid Adv. 6:100254. doi:10.1016/j.hybadv.2024.100254 (2024).

[48]. Djama, C.; Bouguettoucha, A.; Chebli, D.; Amrane, A.; Tahraoui, H.; Zhang, J.; Mouni, L. Experimental and Theoretical Study of Methylene Blue Adsorption on a New Raw Material, *Cynara scolymus*—A Statistical Physics Assessment. *Sustainability 15*, 10364. https://doi.org/ 10.3390/su15131036 (2023).

[49] El-Bery HM, Saleh M, El-Gendy RA, *et al*. High adsorption capacity of phenol and methylene blue using activated carbon derived from lignocellulosic agriculture wastes. Sci Rep. 2022;12:5499. doi:10.1038/s41598-022-09475-4

[50] Lütke SF, Igansi AV, Pegoraro L, *et al*. Preparation of Activated Carbon from Black Wattle Bark Waste and Its Application for Phenol Adsorption. J Environ Chem Eng. 2019;7:103396. doi:10.1016/j.jece.2019.103396

[51] Ngueagni PT, Hefnawy M, Ofudje EA, *et al*. Cellulose-based adsorbent of animal waste for the adsorption of lead and phenol. BioResources. 2025;20(2):3923–3952. doi: 10.15376/biores.20.2.3923-3952

[52] Abdel-Gawwad HA, Ahmed MS, Mohammed AH, *et al*. Utilization of red clay brick waste in the green preparation of an efficient porous nanocomposite for phenol adsorption: Characterization, experiments and statistical physics treatment. Sustain Chem Pharm. 2023;32:101027. doi:10.1016/j.scp.2023.101027

[53] Yilmaz P, Gunduzm D, Ozbek B. Utilization of low-cost bio-waste adsorbent for methylene blue dye removal from aqueous solutions and optimization of process variables by response surface methodology approach. Desalin Water Treat. 2021;224:367–388. doi:10.5004/dwt.2021.27206

[54] Fseha YH, Shaheen J, Sizirici B. Phenol contaminated municipal wastewater treatment using date palm frond biochar: optimization using response surface methodology. Emerg Contam. 2023;9(1):100202. doi:10.1016/j.emcon.2022.100202.

[55]. Michael-Igolima U., Abbey S.J., Ifelebuegu A.O., and Eyo E.U. Modified orange peel waste as a sustainable material for adsorption of contaminants. *Materials (Basel)*. 16(3):1092. doi: 10.3390/ma16031092 (2023).

[56]. Kumar, L., Yadav, V., Yadav, M., Saini, N., Jagannathan, K., Murugesan, V., and Ezhilselvi, V. Systematic studies on the effect of structural modification of orange

peel for remediation of phenol contaminated water. 95(5): e10872. https://doi.org/10.1002/wer.10872 (2023).

[57]. Tolkou AK, Tsoutsa EK, Kyzas GZ, Katsoyiannis IA. Sustainable use of low-cost adsorbents prepared from waste fruit peels for the removal of selected reactive and basic dyes found in wastewaters. Environ Sci Pollut Res Int. 31(10):14662-14689. doi: 10.1007/s11356-024-31868-3 (2024).

[58]. Liu, L., Feng, B., Rao, Y.Z., Tian, C.S., Gu, Q.X. and Huang, T. Development of Efficient Biochar Produced from Orange Peel for Effective La(III) and Y(III) Adsorption. Adsorption Science & Technology, 2023, 5519783. https://doi.org/10.1155/2023/551978 (2023)

[59]. Rana, S., Rana, R.S. and Suresh. S., Studies of biosorption kinetics of phenol by orange peel and tea waste. *Digest Journal of Nanomaterials and Biostructures* 12(2): 579 – 588 (2017).

[60]. Hasdemir, İ.M., Yılmazoğlu, E., Güngör, S. *et al.* Adsorption of acetic acid onto activated carbons produced from hazelnut shell, orange peel, and melon seeds. *Appl Water Sci* **12**, 271 (2022). https://doi.org/10.1007/s13201-022-01797-y

[61]. Kumar, L., Hakeem, I.G., Yadav, M. *et al.* Adsorption of Aminophenol from Aqueous Solution Using KOH Pretreated Biochar Derived from Orange Peel Pyrolysis: Optimization, Kinetics, and Isotherm study. *Environ. Process.* **12**, 36 (2025). https://doi.org/10.1007/s40710-025-00775-1

[62]. Ali, H. J., Al-Heetim, D.T.A., and Abd Rashid, R. Biochar from Orange (citrus sinensis) Peels by Acid Activation for Methylene Blue Adsorption. *Iran. J. Chem. Chem. Eng.* 38(2), 91-105 (2019).

[63]. Zhou, Y., Zhang, X., Deng, J., et al. Adsorption and mechanism study for phenol removal by 10% CO_2 activated bio-char after acid or alkali pretreatment. Journal of Environmental Management 348, 119317. https://doi.org/10.1016/j.jenvman.2023.119317 (2023)

[64]. Kumar, L., Hakeem, I.G., Varathan, E. *et al.* Adsorption of phenol from aqueous solution using activated char synthesized by one-step and two-step KOH activation and pyrolysis of orange peel. *Water Air Soil Pollut* 236, 803. https://doi.org/10.1007/s11270-025-08431-y (2025)

[65]. Kumar, L., Hakeem, I.G., Yadav, M. *et al.* Adsorption of aminophenol from aqueous solution using KOH pretreated biochar derived from orange peel pyrolysis: Optimization, kinetics, and isotherm study. *Environ. Process.* 12, 36. https://doi.org/10.1007/s40710-025-00775-1 (2025).

[66]. Monica, K., Roopa, D., and Stephan, B. Utilisation of low-cost adsorbent made from agro-waste based material for the removal of phenol from aqueous solutions. *International Journal of Innovative Research of Science, Engineering, and Technology*, 14(7). DOI: 10.15680/IJIRSET.2025.1407022 (2025).